UNSTEADY PRESSURE DROP AND HEAT TRANSFER OF MAGNETOHYDRODYNAMIC ANNULAR TWO-PHASE IN RECTANGULAR CHANNEL

Dhefaf Raisan Faisal, Ahmed M. Abdulhadi
Department of Mathematic, Collage of Science, University of Baghdad. Baghdad-Iraq.

Abstract

An annular two-phase, steady and unsteady, flow model in which a conducting fluid flow under the action of magnetic field is concavely. Two models are presented, in the model one; the magnetic field is perpendicular to the long side of the channel, while in the model two is perpendicular to the short side. Also, we study, to some extent the single-phase liquid flow.

It is found that the motion and heat transfer equations are controlled by different dimensionless parameters namely, Reynolds, Hartmann, Prandtl, and Poiseuille parameters. The Laplace transform technique is used to solve each of the motion and heat transfer equations. The effects of each of dimensionless parameters upon the velocity and heat transfer is analyzed.

A comprehensive study for Model 1, and 2 is given. Also, a comparison study among steady, unsteady, single-phase, two-phase for Model 1, and Model 2 is considered.

الضغط اللامستقر وانتقال الحرارة لحقل جريان ممغنط ثنائي الطور في قناة مستطيلة

ضفاف ريسان فيصل،احمد مولود عبد الهادي
قسم الرياضيات، كلية العلوم، جامعة بغداد.بغداد– العراق.

الخلاصة

في هذا البحث تمت دراسة حقل جريان حلقي ثنائي الطور، مستقر وغير مستقر، يحتوي على مائع قابل للتوصيل تحت تأثير حقل مغناطيسي. قدمنا نموذجين للجريان الحلقي ثنائي الطور، في النموذج الاول كان الحقل المغناطيسي مسلط عموديا على عرض القناة ، بينما في النموذج الثاني كان عموديا على طول القناة . كذلك قمنا بدراسة جريان المائع ذو الطور الواحد. لقد تبين ان معادلة الحركة ومعادلة انتقال الحرارة يحكمها اعداد لا بعدية مختلفة، رينولدز ، هارتمان، براندل، بويزلي. لقد استخدمنا تحويل لابلاس لحل كل من معادلة الحركة ومعادلة انتقال الحرارة. وقمنا بدراسة تأثير كل من الاعداد المذكورة اعلاه على كل من السرعة والحرارة. دراسة موسعة لكل من النموذج الاول والنموذج الثاني قد اعطيت. ومقارنات مختلفة تبين الجريان المستقر واللامستقر، احادي الطور وثنائي الطور لكل من النموذج الاول والنموذج الثاني قد قدمت.

Introduction

Magnetofluiddynamics (MFD) is that branch of applied mathematics which deals with the flow of electrically conducting fluids in electric and magnetic fields. It unified in a common framework the electromagnetic and fluid-dynamic theories to yield a description of the

concurrent effects of the magnetic field on the flow and the flow on the magnetic field.

For two-phase flow in a rectangular channel, Thome [1], reported, by performing experiments on gas-liquid metal two-phase flow and developing a homogeneous two-phase flow model that the magnetohydrodynamic MHD pressure drop of two-phase flow is nearly equal to and a little higher than that of single-phase flow, for the same liquid flow rate and the same magnetic field, in the cases of low and medium void fractions. Also, for two-phase flow in a rectangular channel, Owen et al. [2], proposed a separated two-phase flow (annular two-phase flow) model, together with a homogeneous flow model, and showed that the two-phase flow pressure drop cannot be lowered below the single-phase flow pressure drop. However, Inoue et al. [3], showed, by performing experiments on gas-liquid metal two-phase flow that the two-phase flow pressure drop becomes 10 % of the single-phase flow pressure drop in a rectangular channel for the case of high void fraction.

Kumamaru and Fujiwara [4], considered a separated flow (annular flow) models for a rectangular channel have been developed in order to propose a flow model which can predict Inoue et al., experimental data on the magnetohydrodynamic MHD pressure drop. Also, in his work, the heat transfer from the channel walls to gas-liquid metal two-phase flow has been calculated based on the proposed flow models in order to estimate the improvement of heat transfer in the two-phase flow comparing with that in the single-phase liquid flow.

In this paper, the magnetohydrodynamic MHD pressure drop and heat transfer of two-phase flow for fusion reactor conditions have been calculated by the proposed flow and heat transfer models and have been compared with those of single-phase liquid flow.

1. Formulation of the Problems

In this section, we will describe two problems in magnatohydrodynamic MHD namely, Model 1 and Model 2. In both models two-phase gas-liquid flow under the action of uniform magnetic field is considered. The difference between the two problems is in the applied magnetic field.

1.1 Model 1, [5]

In this model, a rectangular channel, an annular two-phase flow (gas-liquid) models has been presented, in which there is a liquid continua adjacent to the channel walls, while in the center of the channel there is a gas continuum. The applied uniform magnetic field, **B**, is directed perpendicularly to the long side of the channel cross-section. Since the flow will be considered in the direction of z-axis, then the applied magnetic field has only one component in the y-direction, this component will be, denoted by B_0, see (figure 1). The paths of induced current for this model flow are in the x-direction and they are shown in (figure 2).

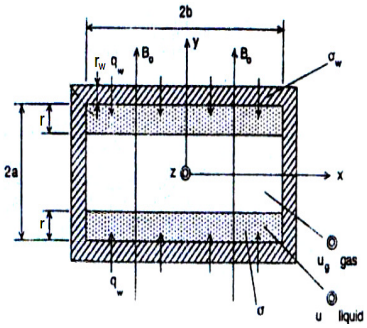

Figure 1: Model 1, annular flow in magnetic field perpendicular to channel long-side, [4].

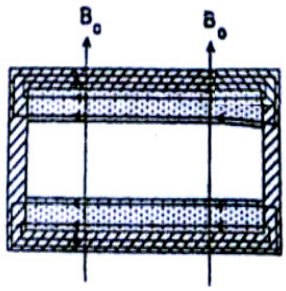

Figure 2: Induced electric current paths in Model 1, [4].

Let a be the half width of short side of the channel and b be the half width of long side of the channel.

1.1.1 Momentum Equation for the Liquid Phase, [4]:

The motion of a conducting liquid under a magnetic field is described by the momentum equation including the Lorentz force (electromagnetic force) term (**J**×**B**) and Ohm's law Thome [1]. They are, respectively, expressed by:

$$\rho\left(\frac{\partial \mathbf{u}}{\partial t}+\mathbf{u}\frac{\partial \mathbf{u}}{\partial z}\right)=-\nabla \mathbf{p}+\mu\nabla^2\mathbf{u}+\mathbf{J}\times\mathbf{B} \qquad \ldots(1)$$

$$\mathbf{J}=\sigma(\mathbf{E}+\mathbf{u}\times\mathbf{B}) \qquad \ldots(2)$$

where, **u** is velocity, **p** is pressure, μ is dynamic viscosity, ρ is density, σ is electrical conductivity, **J** is induced current, **E** is induced electric field, and **B** is magnetic field.

Now, since the flow is unidirectional, in the z-direction, then **u** and $-\nabla \mathbf{p}$ have only z-component, i.e. in the z-direction, let there components be u and ∇ p respectively,.Since the magnatic field **B** in the y-direction, then (**u**×**B**) will be in the x-direction this component say B_0, also we have **E** in the x-direction, consequently **J** will have only one component which is in the x-direction.The total induced current in the x-direction within the liquid is obtained by integration of Eq.(2). **E** in the x-direction is constant, since there is no current in the y-direction.To calculate the last term in the right hand side in Eq(1), we start with Ohm's law:

$$\int_{a-r}^{a} \mathbf{J}\, dy = \int_{a-r}^{a} \sigma(\mathbf{E}+\mathbf{u}\times\mathbf{B})\, dy \qquad \ldots(3)$$

The substitution in Eq(3) performed the integral by using the mean value theorem for integration, we obtain:

$$Jr = r\sigma E - r\sigma \bar{u} B_0$$

where, B_0 the applied magnetic field, and $\bar{u}$ is the average liquid velocity. The plus and minus signs correspond to the positive and negative direction of the y-axis, respectively. The total current in the x-direction within the wall is given by:

$$J_w r_w = r_w \sigma_w E$$

where, J_w is the wall induced current, r_w is the wall thickness, σ_w is the wall electrical conductivity.The application of the continuously equation for current tell us that the net current in the x-direction must be zero, i.e.,

$$r\sigma(E - \bar{u} B_0) + r_w \sigma_w E = 0$$

from which

$$E = \frac{\bar{u} B_0}{1 + r_w \sigma_w / r\sigma} \qquad \ldots(4)$$

Let $\gamma = (a - r)/a$, and the wall conductivity number $\phi = \frac{r_w \sigma_w}{a\sigma}$ .Then Eq.(4) becomes:

$$E = \frac{\bar{u} B_0}{1 + \phi/(1-\gamma)}$$

where, γ is a void fraction.

By substituting the above expression for E in Ohm's law, Eq.(2), we get:

$$J = \sigma(E - \bar{u} B_0)$$

$$J = \frac{\sigma \bar{u} B_0}{1 + \phi/(1-\gamma)} - \sigma u B_0$$

Now, we have:

$$(\mathbf{J}\times\mathbf{B}) = \left(\frac{\sigma \bar{u} B_0^2}{1 + \phi/(1-\gamma)} - \sigma u B_0^2 \right)$$

The substituting of the last equation in the momentum Eq.(1) gives final form of momentum equation, which is:

$$\rho\left(\frac{\partial u}{\partial t}\right) = -\frac{\partial P}{\partial z} + \mu \frac{\partial^2 u}{\partial y^2} + \frac{\sigma \bar{u} B_0^2}{1 + \phi/(1-\gamma)} - \sigma u B_0^2 . \qquad (5)$$

The associated boundary conditions are:

$u = 0$ at $y = a$ (non-slip condition) …(6a)

and,

$$-\mu \frac{\partial u}{\partial y} = \tau_l = (a - r)\left(-\frac{\partial P}{\partial z}\right) \text{ at } y = a - r \quad \ldots (6b)$$

(viscosity law) and the initial condition:

$u = 0$ at $t = 0$ …(6c)

Note that, Eq.(5) and its boundary conditions are in dimensional form.

1.1.2 Gas-Phase, [4]:

For the gas phase with a large gas-to-liquid relative velocity, the pressure gradient, Branover [5], is evaluated for a flow channel with a width of 2a, is given by:

$$\frac{-\partial P/\partial z}{\rho_g \bar{u}_g^2 / 2a} = f$$

Now, since in our case, the channel width is 2a − 2r, thus we have:

$$-\frac{\partial P}{\partial z} = f \frac{\rho_g \bar{u}_g^2}{2(a-r)}$$

$$-\frac{\partial P}{\partial z} = 4f \frac{1}{d_h} \frac{\rho_g \bar{u}_g^2}{2} \qquad \ldots(7)$$

where, ρ_g is density of gas, $\bar{u}_g$ is the average liquid velocity of gas, and $d_h = 4(a - r)$ is the hydraulic equivalent diameter, defined for the infinite parallel plates and the friction coefficient, f, is evaluated by:

$$\left.\begin{aligned} f &= 16/Re_g \quad \text{for} \quad Re_g \le 2000 \\ f &= 0.0791/Re_g^{0.25} \quad \text{for} \quad Re_g \ge 2000 \end{aligned}\right\} \quad \ldots(8\ a,b)$$

The Reynolds numbers, based on both real velocities and superficial velocities, are defined by using the hydraulic equivalent diameters for the infinite parallel plates.

$$\bar{u} = \frac{\bar{u}_0}{1-\gamma} \qquad \ldots(9\ a)$$

$$\bar{u}_g = \frac{\bar{u}_{g_0}}{\gamma} \qquad \ldots(9\ b)$$

$$\left.\begin{aligned} Re &= \rho \bar{u} 4r/\mu, \qquad Re_g = \rho_g \bar{u}_g 4(a-r)/\mu_g \\ Re_0 &= \rho \bar{u}_0 4a/\mu (= Re), Re_{g_0} = \rho_g \bar{u}_{g_0} 4a/\mu_g (= Re_g) \end{aligned}\right\}$$

…(10 a,b,c,d)

where μ_g is the dynamic viscosity of the gas.

The average velocity is given by :

$$\bar{u} = \frac{1}{r}\int_{a-r}^{a} u\, dy \qquad \ldots(11)$$

By introducing the nondimensional new variables $u^* = u/\bar{u}$, $y^* = y/a$, Hartmann number $Ha = B_0 a\sqrt{\sigma/\mu}$, Poiseuille number $P = \left(-\frac{\partial P}{\partial z}\right)\left(\frac{a^2}{\mu\bar{u}}\right)$ and $t^* = \frac{t\bar{u}}{4a}$, the momentum equation in dimensionless form can be written as

$$\frac{1}{16}Re_0\frac{\partial u^*}{\partial t^*} = P + \frac{\partial^2 u^*}{\partial y^{*2}} + \frac{Ha^2}{1+\phi/(1-\gamma)} - Ha^2 u^* \qquad \ldots(12)$$

The associated boundary and the initial conditions are:

$$u^* = 0 \text{ at } y^* = 1,\ -\frac{\partial u^*}{\partial y^*} = \gamma P \text{ at } y^* = \gamma,$$

$$u^* = 0 \text{ at } t^* = 0 \qquad \ldots(13a,b,c)$$

1.2 Energy Equation, [4]

By neglecting the internal heat generation for the present one-dimensional problem, the unsteady state energy equation for liquid phase with a constant heat flux from long-side channel wall for this model is:

$$\rho C_p\left(\frac{\partial\theta}{\partial t} + u\frac{\partial\theta}{\partial z}\right) = k\frac{\partial^2\theta}{\partial y^2} \qquad \ldots(14)$$

where C_p is specific heat, θ is temperature, θ_w is temperature of the wall, $\theta^* = \theta - \theta_w$, k is thermal conductivity.

The associated boundary and initial conditions are:

$$\theta = \theta_w \text{ at } y = a,\ \frac{\partial\theta}{\partial y} = 0 \text{ at } y = a - r$$

$$, \theta = 0 \text{ at } t = 0 \qquad \ldots(15a,b,c)$$

By introducing nondimensional variables $u^* = u/\bar{u}$, $y^* = y/a$, and $z^* = z/a$, $t^* = \frac{t\bar{u}}{4a}$, and Prandtl number $Pr = \frac{\mu C_p}{k}$.

$$\frac{\partial^2\theta^*}{\partial y^{*2}} = \frac{1}{4}\frac{Re_0 Pr}{4(1-\gamma)}\frac{\partial\theta^*}{\partial t^*} + \frac{Re_0 Pr}{4(1-\gamma)}u^*\frac{\partial\theta}{\partial z^*} \qquad \ldots(16)$$

and $\frac{\partial\theta}{\partial z^*}$ is constant, because of constant wall heat flux.

The associated boundary and initial conditions are:

$$\theta^* = 0 \text{ at } y^* = 1,\ \frac{\partial\theta^*}{\partial y^*} = 0 \text{ at } y^* = \gamma,$$

$$\theta^* = 0 \text{ at } t^* = 0 \qquad \ldots(17a,b,c)$$

The dimensionless form of equation (7) can be written as:

$$P = f\frac{Re_{g_0}^2}{d_h}\frac{\mu}{\rho\bar{u}_0 4a}\frac{\bar{u}_g^2\bar{u}_0 4a}{8\bar{u}_{g_0}^2\bar{u}}\left(\frac{\rho}{\rho_g}\right)\left(\frac{\mu_g}{\mu}\right)^2$$

By using the equations $d_h = 4(a - r)$, $\bar{u}_g = \bar{u}_{g_0}/\gamma$, and $\bar{u} = \bar{u}_0/(1-\gamma)$, we get:

$$P = f\frac{Re_{g_0}^2}{Re_0}\frac{\rho}{\rho_g}\left(\frac{\mu_g}{\mu}\right)^2\frac{1-\gamma}{\gamma^3}\frac{1}{8} \qquad \ldots(18)$$

The dimensionless form of equation (8a,b) can be written as:

$$\left.\begin{aligned} f &= 16/Re_{g_0} \quad \text{for } Re_{g_0} \le 2000 \\ f &= 0.0791/Re_{g_0}^{0.25} \quad \text{for } Re_{g_0} \ge 2000 \end{aligned}\right\} \ldots(19\ a,b)$$

By using the same procedure, the dimensionless form of the average velocity ,equation 11, is:

$$1 = \frac{1}{1-\gamma}\int_{\gamma}^{1} u^*\, dy^* \qquad \ldots(20)$$

1.3 Model 2, [4]

In this model, a rectangular channel, an annular two-phase flow (gas-liquid) models has been presented, in which there is a liquid continua adjacent to the channel walls, while in the center of the channel there is a gas continuum. The applied uniform magnetic field, **B**, is directed perpendicularly to the short side of the channel cross-section. Since the flow will be considered in the direction of z-axis, then the applied magnetic field has only one component in the x-direction, this component will be, denoted by B_0, see (figure 3). The paths of induced current for this model flow are in the y-direction and they are shown in (figure 4).

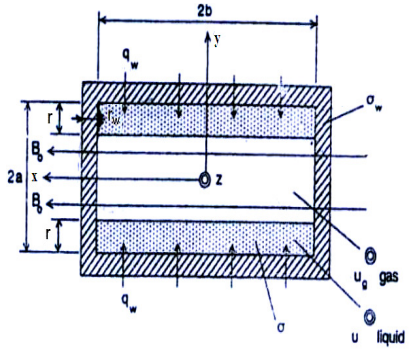

Figure 3: Model 2, annular flow in magnetic field perpendicular to channel short side, [4].

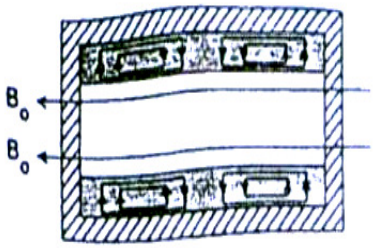

Figure 4: Induced electric current paths in Model 2, [4].

Let a be the half width of short side of the channel and b be the half width of long side of the channel. In Model 2, one side of the liquid film is in contact with gas core, i.e., nonconducting medium, and the thickness of channel wall perpendicular to the magnetic field, r_w is considerably smaller than the half width of the channel parallel to the magnetic field, **B**. Hence, induced current paths are considered to be nearly equivalent to those for liquid flow in a channel insulating (nonconducting) walls perpendicular to the magnetic field Lielausis [6]. From the above consideration, the equations as for Model 1 hold for Model 2 except that the coordinate y and y* replaced by x and x*, respectively, and conductivity number ϕ is set to be zero.

The momentum equation is:

$$\rho\left(\frac{\partial u}{\partial t}\right)=-\frac{\partial P}{\partial z}+\mu\frac{\partial^2 u}{\partial x^2}-\sigma B_0^2(u-\bar{u}) \qquad \ldots(21)$$

The associated boundary conditions are:

$u = 0$ at $x = a$ (Non-Slip condition) …(22a)

and

$$-\mu\frac{\partial u}{\partial x}=\tau_1=(a-r)\left(-\frac{\partial P}{\partial z}\right) \quad \text{at} \quad x = a - r$$

(Viscosity Law) …(22b)

and the initial condition:

$u = 0$ at $t = 0$ …(22c)

The energy equation is:

$$\rho C_p\left(\frac{\partial\theta}{\partial t}+u\frac{\partial\theta}{\partial z}\right)=k\frac{\partial^2\theta}{\partial x^2} \qquad \ldots(23)$$

The associated boundary and initial conditions are:

$$\theta=\theta_w \text{ at } x=a\ , \qquad \frac{\partial\theta}{\partial x}=0 \text{ at } x=a-r,$$

$\theta = 0$ at $t = 0$ …(24a,b,c)

Then the momentum and energy equations in dimensionless form are:

$$\frac{1}{16}\mathrm{Re}_0\frac{\partial u^*}{\partial t^*}=P+\frac{\partial^2 u^*}{\partial x^{*2}}+Ha^2-Ha^2u^* \qquad \ldots(25)$$

The associated boundary and initial condition can be written as:

$$u^*=0 \text{ at } x^*=1\ , \quad -\frac{\partial u^*}{\partial x^*}=\gamma P \text{ at } x^*=\gamma,$$

$u^* = 0$ at $x^* = 0$ …(26a,b,c)

The energy equations is:

$$\frac{\partial^2\theta^*}{\partial x^{*2}}=\frac{1}{4}\frac{\mathrm{Re}_0\,\mathrm{Pr}}{4(1-\gamma)}\frac{\partial\theta^*}{\partial t^*}+\frac{\mathrm{Re}_0\,\mathrm{Pr}}{4(1-\gamma)}u^*\frac{\partial\theta}{\partial z^*} \qquad \ldots(27)$$

and $\frac{\partial\theta}{\partial z^*}$ is constant, because of constant wall heat flux.

The associated boundary and initial conditions can be written as:

$$\theta^*=0 \text{ at } x^*=1, \qquad \frac{\partial\theta^*}{\partial x^*}=0 \text{ at } x^*=\gamma,$$

$\theta^* = 0$ at $t^* = 0$ …(28a,b,c)

2. Solution of the Problems

In this section, we will describe the solution of Model 1 and Model 2. The Laplace transformation method is used to solve these problems.

2.1 The Solution of Model 1

The solution of velocity equation is:

$$u^*(y^*,s)=\frac{\gamma P\sinh\{Ha(1-y^*)\}}{Ha\cosh\{Ha(1-\gamma)\}}-\frac{P'\cosh\{Ha(y^*-\gamma)\}}{Ha^2\cosh\{Ha(1-\gamma)\}}+\frac{P'}{Ha^2}+\frac{32\gamma Pe^{\ell t}\sinh\{M(1-y^*)\}}{\mathrm{Re}_0(1-\gamma)\ell\sinh\{M(1-\gamma)\}}-\frac{32P'e^{\ell t}\cosh\{M(y^*-\gamma)\}}{\mathrm{Re}_0(1-\gamma)\ell M\sinh\{M(1-\gamma)\}} \qquad \ldots(29)$$

where:

$$\ell=\sum_{n=1}^{\infty}\frac{-4(2n+1)^2\pi^2}{(1-\gamma)^2\,\mathrm{Re}_0}-\frac{16Ha^2}{\mathrm{Re}_0},$$

$$M=\sqrt{\frac{1}{16}\mathrm{Re}_0\,\ell+Ha^2}\ , \text{ and}$$

$$P'=\frac{Ha^2}{1+\phi/(1-\gamma)}+P \qquad \ldots(30)$$

From expression (30), one can see that the velocity distribution is depending on y-coordinate and time t, also it depends on the dimensionless numbers Re_0, P, and Ha. It is easy to show that the u*-solution for unsteady state (30) approaches the u*-solution for steady state as t approaches infinity, which is:

$$u^* = \frac{\gamma P \sinh\{Ha(1-y^*)\}}{Ha\cosh\{Ha(1-\gamma)\}} - \frac{P'\cosh\{Ha(y^*-\gamma)\}}{Ha^2\cosh\{Ha(1-\gamma)\}} + \frac{P'}{Ha^2} \quad \ldots(31)$$

The last solution is corresponding to steady case as in [4].

2.1.1 Friction Pressure Drop (Poiseuille Number):

By substituting equation (31) in equation (20), the friction pressure drop in nondimensional form, i.e., the Poiseuille number result in:

$$P = \frac{Ha^2}{1+\phi/(1-\gamma)}[\phi Ha \cosh\{Ha(1-\gamma)\} Re_0(1-\gamma)\ell M^2\sinh\{M(1-\gamma)\} + 32\,e^{\ell t} Ha^3\cosh\{Ha(1-\gamma)\}\sinh\{M(1-\gamma)\} + Re_0(1-\gamma)\ell M^2\sinh\{Ha(1-\gamma)\}\sinh\{M(1-\gamma)\}] \Big/ [(M^2 Re_0(1-\gamma)\ell \sinh\{M(1-\gamma)\})(Ha\cosh\{Ha(1-\gamma)\} - \gamma Ha - \sinh\{Ha(1-\gamma)\} - 32\gamma M\,e^{\ell t} Ha^3\cosh\{Ha(1-\gamma)\}(1-\cosh\{M(1-\gamma)\}) - 32\,e^{\ell t} Ha^3\cosh\{Ha(1-\gamma)\}\sinh\{M(1-\gamma)\}] \quad \ldots(32)$$

Now, for large Hartmann number, it is easy to show that the Poiseuille number for unsteady state (32) approaches the Poiseuille number for steady state as t approaches infinity, which is:

$$P = Ha^2\left\{\frac{\phi}{1+\frac{\phi}{1-\gamma}} + \frac{1}{Ha}\frac{1+\phi}{1+\frac{\phi}{1-\gamma}}\right\}, \gamma \neq 0 \quad \ldots(33)$$

The last solution is corresponding to steady case as in [4].

The solution of energy equation is:

$$\theta^*(y^*,s) = \frac{Re_0 Pr}{4(1-\gamma)}\frac{\partial\theta}{\partial z^*}\left[\frac{\gamma P}{Ha^3}\frac{\sinh\{Ha(1-y^*)\}}{\cosh\{Ha(1-\gamma)\}} - \frac{P'}{Ha^4}\frac{\cosh\{Ha(y^*-\gamma)\}}{\cosh\{Ha(1-\gamma)\}} + \frac{P'}{2Ha^2}y^{*2} + \frac{\gamma}{Ha^2}(P - P')y^* - \frac{\gamma P}{Ha^2} + \frac{P'}{Ha^4} + \frac{P'}{Ha^2}\left(\gamma-\frac{1}{2}\right)\right] + 128\frac{\partial\theta}{\partial z^*}\frac{P'}{Ha^2}$$

$$\frac{\exp\left(\sum_{n=1}^{\infty}-\frac{4(2n+1)^2\pi^2}{Re_0 Pr(1-\gamma)}t\right)\cosh\left\{\sqrt{\sum_{n=1}^{\infty}-\frac{(2n+1)^2\pi^2}{4(1-\gamma)^2}}(y^*-\gamma)\right\}}{\sum_{n=1}^{\infty}\frac{\left(-4(2n+1)^2\pi^2\right)^2}{Re_0 Pr(1-\gamma)^2}} \frac{\sqrt{\sum_{n=1}^{\infty}-\frac{(2n+1)^2\pi^2}{4(1-\gamma)^2}}}{\sinh\left\{\sqrt{\sum_{n=1}^{\infty}-\frac{(2n+1)^2\pi^2}{4(1-\gamma)^2}}(1-\gamma)\right\}} +$$

$$128\frac{\partial\theta}{\partial z^*}\frac{P'}{Ha^2}\frac{\exp\left(\sum_{n=1}^{\infty}-\frac{4(2n+1)^2\pi^2}{Re_0 Pr(1-\gamma)}t\right)\cosh\left\{\sqrt{\sum_{n=1}^{\infty}-\frac{(2n+1)^2\pi^2}{4(1-\gamma)^2}}(y^*-\gamma)\right\}}{\sum_{n=1}^{\infty}\left(\frac{-4(2n+1)^2\pi^2}{(1-\gamma)}\right)\left(\frac{16Ha^2(1-\gamma)}{Re_0 Pr}-\left(\sum_{n=1}^{\infty}\frac{-4(2n+1)^2\pi^2}{Re_0 Pr(1-\gamma)}\right)\right)} \frac{\sqrt{\sum_{n=1}^{\infty}-\frac{(2n+1)^2\pi^2}{4(1-\gamma)^2}}}{\sinh\left\{\sqrt{\sum_{n=1}^{\infty}-\frac{(2n+1)^2\pi^2}{4(1-\gamma)^2}}(1-\gamma)\right\}} + \frac{\partial\theta}{\partial z^*}\frac{128P'\cosh\{M(1-\gamma)\}}{Re_0(1-\gamma)\ell M\sinh\{M(1-\gamma)\}}$$

$$\frac{\cosh\left\{\sqrt{\frac{\ell}{4}\frac{Re_0 Pr}{4(1-\gamma)}}(y^*-\gamma)\right\}e^{\ell t}}{\left(\frac{16M^2(1-\gamma)}{Re_0 Pr}-\ell\right)\cosh\left\{\sqrt{\frac{\ell}{4}\frac{Re_0 Pr}{4(1-\gamma)}}(1-\gamma)\right\}} + 4096\frac{\partial\theta}{\partial z^*}\frac{P'\cosh\{M(1-\gamma)\}}{Re_0(1-\gamma)M\ell\sinh\{M(1-\gamma)\}}$$

$$\frac{\exp\left(\sum_{n=1}^{\infty}-\frac{4(2n+1)^2\pi^2}{Re_0 Pr(1-\gamma)}t\right)\cosh\left\{\sqrt{\sum_{n=1}^{\infty}-\frac{(2n+1)^2\pi^2}{4(1-\gamma)^2}}(y^*-\gamma)\right\}}{\left(\sum_{n=1}^{\infty}\frac{-4(2n+1)^2\pi^2}{Re_0 Pr(1-\gamma)}-\ell\right)Re_0 Pr\left(\frac{16M^2(1-\gamma)}{Re_0 Pr}-\left(\sum_{n=1}^{\infty}\frac{-4(2n+1)^2\pi^2}{Re_0 Pr(1-\gamma)}\right)\right)} \frac{\sqrt{\sum_{n=1}^{\infty}-\frac{(2n+1)^2\pi^2}{4(1-\gamma)^2}}}{\sinh\left\{\sqrt{\sum_{n=1}^{\infty}-\frac{(2n+1)^2\pi^2}{4(1-\gamma)^2}}(1-\gamma)\right\}} - 128\frac{\partial\theta}{\partial z^*}\gamma P$$

$$\frac{\exp\left(\sum_{n=1}^{\infty}-\frac{4(2n+1)^2\pi^2}{Re_0 Pr(1-\gamma)}t\right)\sinh\left\{\sqrt{\sum_{n=1}^{\infty}-\frac{(2n+1)^2\pi^2}{4(1-\gamma)^2}}(1-y^*)\right\}}{\sum_{n=1}^{\infty}\left(\frac{-4(2n+1)^2\pi^2}{(1-\gamma)}\right)\left(\frac{16Ha^2(1-\gamma)}{Re_0 Pr}-\left(\sum_{n=1}^{\infty}\frac{-4(2n+1)^2\pi^2}{Re_0 Pr(1-\gamma)}\right)\right)} \frac{1}{\sinh\left\{\sqrt{\sum_{n=1}^{\infty}-\frac{(2n+1)^2\pi^2}{4(1-\gamma)^2}}(1-\gamma)\right\}} -$$

$$128\frac{\partial\theta}{\partial z^*}\frac{\gamma PM\cosh\{M(1-\gamma)\}}{Re_0(1-\gamma)\ell\sinh\{M(1-\gamma)\}}$$

$$\frac{\sinh\left\{\sqrt{\frac{\ell}{4}\frac{\mathrm{Re_0\,Pr}}{4(1-\gamma)}}(1-y^*)\right\}e^{\ell t}}{\left(\frac{16M^2(1-\gamma)}{\mathrm{Re_0\,Pr}}-\ell\right)\sqrt{\frac{\ell}{4}\frac{\mathrm{Re_0\,Pr}}{4(1-\gamma)}}\cosh\left\{\sqrt{\frac{\ell}{4}\frac{\mathrm{Re_0\,Pr}}{4(1-\gamma)}}(1-\gamma)\right\}} -$$

$$4096\frac{\partial\theta}{\partial z^*}\frac{\gamma PM\cosh\{M(1-\gamma)\}}{\mathrm{Re_0}(1-\gamma)\ell\sinh\{M(1-\gamma)\}}$$

$$\frac{\exp\left(\sum_{n=1}^{\infty}-\frac{4(2n+1)^2\pi^2}{\mathrm{Re_0\,Pr}(1-\gamma)}t\right)}{\mathrm{Re_0\,Pr}\left(\sum_{n=1}^{\infty}\frac{-4(2n+1)^2\pi^2}{\mathrm{Re_0\,Pr}(1-\gamma)}-\ell\right)\left(\frac{16M^2(1-\gamma)}{\mathrm{Re_0\,Pr}}-\left(\sum_{n=1}^{\infty}\frac{-4(2n+1)^2\pi^2}{\mathrm{Re_0\,Pr}(1-\gamma)}\right)\right)}$$

$$\frac{\sinh\left\{\sqrt{\sum_{n=1}^{\infty}-\frac{(2n+1)^2\pi^2}{4(1-\gamma)^2}}(1-y^*)\right\}}{\sinh\left\{\sqrt{\sum_{n=1}^{\infty}-\frac{(2n+1)^2\pi^2}{4(1-\gamma)^2}}(1-\gamma)\right\}}+128\frac{\partial\theta}{\partial z^*}$$

$$\frac{\gamma P\sinh\{M(1-y^*)\}e^{\ell t}}{(1-\gamma)\ell\sinh\{M(1-\gamma)\}}\quad\frac{\mathrm{Pr}}{16M^2(1-\gamma)-\mathrm{Re_0\,Pr}\,\ell}$$

$$-128\frac{\partial\theta}{\partial z^*}\frac{P'\cosh\{M(y^*-\gamma)\}e^{\ell t}}{(1-\gamma)\ell M\sinh\{M(1-\gamma)\}}$$

$$\frac{\mathrm{Pr}}{16M^2(1-\gamma)-\mathrm{Re_0\,Pr}\,\ell}\qquad\ldots(34)$$

From expression (34), one can see that the temperature distribution is depending on y-coordinate and time t, also it depends on the dimensionless numbers $\mathrm{Re_0}$, P, Ha and Pr. It is easy to show that θ*-solution for unsteady state (34) approaches the θ*-solution for steady state as t approaches infinity, which is:

$$\theta^* = \frac{\mathrm{Re_0\,Pr}}{4(1-\gamma)}\frac{\partial\theta}{\partial z^*}\left[\frac{\gamma P}{Ha^3}\frac{\sinh\{Ha(1-y^*)\}}{\cosh\{Ha(1-\gamma)\}}-\frac{P'}{Ha^4}\right.$$

$$\frac{\cosh\{Ha(y^*-\gamma)\}}{\cosh\{Ha(1-\gamma)\}}+\frac{P'}{2Ha^2}y^{*2}+\frac{\gamma}{Ha^2}(P-$$

$$\left.P')y^*-\frac{\gamma P}{Ha^2}+\frac{P'}{Ha^4}+\frac{P'}{Ha^2}\left(\gamma-\frac{1}{2}\right)\right]\ldots(35)$$

The last solution is corresponding to steady case as in [4].

2.2 The Solution of Model 2

The solution of velocity and energy equations are:

$$u^*(x^*,s)=\frac{\gamma P\sinh\{Ha(1-x^*)\}}{Ha\cosh\{Ha(1-\gamma)\}}-\frac{P'\cosh\{Ha(x^*-\gamma)\}}{Ha^2\cosh\{Ha(1-\gamma)\}}$$

$$+\frac{P'}{Ha^2}+\frac{32\gamma Pe^{\ell t}\sinh\{M(1-x^*)\}}{\mathrm{Re_0}(1-\gamma)\ell\sinh\{M(1-\gamma)\}}$$

$$\frac{32P'e^{\ell t}\cosh\{M(x^*-\gamma)\}}{\mathrm{Re_0}(1-\gamma)\ell M\sinh\{M(1-\gamma)\}}\qquad\ldots(36)$$

where:

$$P'=P+Ha^2,\ \ell=\sum_{n=1}^{\infty}\frac{-4(2n+1)^2\pi^2}{(1-\gamma)^2\,\mathrm{Re_0}}-\frac{16Ha^2}{\mathrm{Re_0}},\text{ and}$$

$$M=\sqrt{\frac{1}{16}\mathrm{Re_0}\,\ell+Ha^2}$$

and the solution of heat equation (27), is:

$$\theta^*(x^*,s)=\frac{\mathrm{Re_0\,Pr}}{4(1-\gamma)}\frac{\partial\theta}{\partial z^*}\left[\frac{\gamma P}{Ha^3}\frac{\sinh\{Ha(1-x^*)\}}{\cosh\{Ha(1-\gamma)\}}-\frac{P'}{Ha^4}\right.$$

$$\frac{\cosh\{Ha(x^*-\gamma)\}}{\cosh\{Ha(1-\gamma)\}}+\frac{P'}{2Ha^2}x^{*2}+\frac{\gamma}{Ha^2}$$

$$(P-P')x^*-\frac{\gamma P}{Ha^2}+\frac{P'}{Ha^4}+\frac{P'}{Ha^2}\left(\gamma-\frac{1}{2}\right)\Bigg]+$$

$$128\frac{\partial\theta}{\partial z^*}\frac{P'}{Ha^2}$$

$$\frac{\exp\left(\sum_{n=1}^{\infty}-\frac{4(2n+1)^2\pi^2}{\mathrm{Re_0\,Pr}(1-\gamma)}t\right)\cosh\left\{\sqrt{-\sum_{n=1}^{\infty}\frac{(2n+1)^2\pi^2}{4(1-\gamma)^2}}(x^*-\gamma)\right\}}{\sum_{n=1}^{\infty}\frac{\left(-4(2n+1)^2\pi^2\right)^2}{\mathrm{Re_0\,Pr}(1-\gamma)^2}}$$

$$\frac{\sqrt{\sum_{n=1}^{\infty}-\frac{(2n+1)^2\pi^2}{4(1-\gamma)^2}}}{\sinh\left\{\sqrt{\sum_{n=1}^{\infty}-\frac{(2n+1)^2\pi^2}{4(1-\gamma)^2}}(1-\gamma)\right\}}+128\frac{\partial\theta}{\partial z^*}\frac{P'}{Ha^2}$$

$$\frac{\exp\left(\sum_{n=1}^{\infty}-\frac{4(2n+1)^2\pi^2}{\mathrm{Re_0\,Pr}(1-\gamma)}t\right)\cosh\left\{\sqrt{\sum_{n=1}^{\infty}-\frac{(2n+1)^2\pi^2}{4(1-\gamma)^2}}(x^*-\gamma)\right\}}{\sum_{n=1}^{\infty}\left(\frac{-4(2n+1)^2\pi^2}{(1-\gamma)}\right)\left(\frac{16Ha^2(1-\gamma)}{\mathrm{Re_0\,Pr}}-\left(\sum_{n=1}^{\infty}\frac{-4(2n+1)^2\pi^2}{\mathrm{Re_0\,Pr}(1-\gamma)}\right)\right)}$$

$$\frac{\sqrt{\sum_{n=1}^{\infty}-\frac{(2n+1)^2\pi^2}{4(1-\gamma)^2}}}{\sinh\left\{\sqrt{\sum_{n=1}^{\infty}-\frac{(2n+1)^2\pi^2}{4(1-\gamma)^2}}(1-\gamma)\right\}}+$$

$$\frac{\partial\theta}{\partial z^*}\frac{128P'\cosh\{M(1-\gamma)\}}{\mathrm{Re_0}(1-\gamma)\ell M\sinh\{M(1-\gamma)\}}$$

$$\frac{\cosh\left\{\sqrt{\frac{\ell}{4}\frac{\mathrm{Re_0\,Pr}}{4(1-\gamma)}}(x^*-\gamma)\right\}e^{\ell t}}{\left(\frac{16M^2(1-\gamma)}{\mathrm{Re_0\,Pr}}-\ell\right)\cosh\left\{\sqrt{\frac{\ell}{4}\frac{\mathrm{Re_0\,Pr}}{4(1-\gamma)}}(1-\gamma)\right\}}+$$

$$4096\frac{\partial\theta}{\partial z^*}\frac{P'\cosh\{M(1-\gamma)\}}{\mathrm{Re_0}(1-\gamma)M\ell\sinh\{M(1-\gamma)\}}$$

$$\frac{\exp\left(\sum_{n=1}^{\infty}-\frac{4(2n+1)^2\pi^2}{\mathrm{Re_0\,Pr}(1-\gamma)}t\right)\cosh\left\{\sqrt{\sum_{n=1}^{\infty}-\frac{(2n+1)^2\pi^2}{4(1-\gamma)^2}}(x^*-\gamma)\right\}}{\left(\sum_{n=1}^{\infty}\frac{-4(2n+1)^2\pi^2}{\mathrm{Re_0\,Pr}(1-\gamma)}-\ell\right)\mathrm{Re_0\,Pr}\left(\frac{16M^2(1-\gamma)}{\mathrm{Re_0\,Pr}}-\left(\sum_{n=1}^{\infty}\frac{-4(2n+1)^2\pi^2}{\mathrm{Re_0\,Pr}(1-\gamma)}\right)\right)}$$

$$\frac{\sqrt{\sum_{n=1}^{\infty}-\frac{(2n+1)^2\pi^2}{4(1-\gamma)^2}}}{\sinh\left\{\sqrt{\sum_{n=1}^{\infty}-\frac{(2n+1)^2\pi^2}{4(1-\gamma)^2}}(1-\gamma)\right\}}-128\frac{\partial\theta}{\partial z^*}\gamma P$$

$$\frac{\exp\left(\sum_{n=1}^{\infty}-\frac{4(2n+1)^2\pi^2}{\mathrm{Re}_0\,\mathrm{Pr}(1-\gamma)}t\right)}{\sum_{n=1}^{\infty}\left(\frac{-4(2n+1)^2\pi^2}{(1-\gamma)}\right)\left(\frac{16\mathrm{Ha}^2(1-\gamma)}{\mathrm{Re}_0\,\mathrm{Pr}}-\left(\sum_{n=1}^{\infty}\frac{-4(2n+1)^2\pi^2}{\mathrm{Re}_0\,\mathrm{Pr}(1-\gamma)}\right)\right)}$$

$$\frac{\sinh\left\{\sqrt{\sum_{n=1}^{\infty}-\frac{(2n+1)^2\pi^2}{4(1-\gamma)^2}}(1-x^*)\right\}}{\sinh\left\{\sqrt{\sum_{n=1}^{\infty}-\frac{(2n+1)^2\pi^2}{4(1-\gamma)^2}}(1-\gamma)\right\}}-128\frac{\partial\theta}{\partial z^*}$$

$$\frac{\gamma P M\cosh\{M(1-\gamma)\}}{\mathrm{Re}_0(1-\gamma)\ell\sinh\{M(1-\gamma)\}}$$

$$\frac{\sinh\left\{\sqrt{\frac{\ell}{4}\frac{\mathrm{Re}_0\,\mathrm{Pr}}{4(1-\gamma)}}(1-x^*)\right\}e^{\ell t}}{\left(\frac{16M^2(1-\gamma)}{\mathrm{Re}_0\,\mathrm{Pr}}-\ell\right)\sqrt{\frac{\ell}{4}\frac{\mathrm{Re}_0\,\mathrm{Pr}}{4(1-\gamma)}}\cosh\left\{\sqrt{\frac{\ell}{4}\frac{\mathrm{Re}_0\,\mathrm{Pr}}{4(1-\gamma)}}(1-\gamma)\right\}}$$

$$-4096\frac{\partial\theta}{\partial z^*}\frac{\gamma P M\cosh\{M(1-\gamma)\}}{\mathrm{Re}_0(1-\gamma)\ell\sinh\{M(1-\gamma)\}}$$

$$\frac{\exp\left(\sum_{n=1}^{\infty}-\frac{4(2n+1)^2\pi^2}{\mathrm{Re}_0\,\mathrm{Pr}(1-\gamma)}t\right)}{\mathrm{Re}_0\,\mathrm{Pr}\left(\sum_{n=1}^{\infty}\frac{-4(2n+1)^2\pi^2}{\mathrm{Re}_0\,\mathrm{Pr}(1-\gamma)}-\ell\right)\left(\frac{16M^2(1-\gamma)}{\mathrm{Re}_0\,\mathrm{Pr}}-\left(\sum_{n=1}^{\infty}\frac{-4(2n+1)^2\pi^2}{\mathrm{Re}_0\,\mathrm{Pr}(1-\gamma)}\right)\right)}$$

$$\frac{\sinh\left\{\sqrt{\sum_{n=1}^{\infty}-\frac{(2n+1)^2\pi^2}{4(1-\gamma)^2}}(1-x^*)\right\}}{\sinh\left\{\sqrt{\sum_{n=1}^{\infty}-\frac{(2n+1)^2\pi^2}{4(1-\gamma)^2}}(1-\gamma)\right\}}+128\frac{\partial\theta}{\partial z^*}$$

$$\frac{\gamma P\sinh\{M(1-x^*)\}e^{\ell t}}{(1-\gamma)\ell\sinh\{M(1-\gamma)\}}\frac{\mathrm{Pr}}{16M^2(1-\gamma)-\mathrm{Re}_0\,\mathrm{Pr}\,\ell}$$

$$-128\frac{\partial\theta}{\partial z^*}\frac{P'\cosh\{M(x^*-\gamma)\}e^{\ell t}}{(1-\gamma)\ell M\sinh\{M(1-\gamma)\}}$$

$$\frac{\mathrm{Pr}}{16M^2(1-\gamma)-\mathrm{Re}_0\,\mathrm{Pr}\,\ell} \qquad \ldots(37)$$

3. Results and Discussion

In this section, we have studied the effect of different parameters that governing the motion and energy equations, upon the velocity distribution and heat transfer.

3.1 Velocity Distribution of Model 1

In this section, we have studied the effect of Reynolds, Hartmann numbers, and time will be considered also.

Effect of Reynolds number, To study the effect of Reynolds number on the velocity distribution, we keep Hartmann number and time fixed at 469, Pi/4 and we give Reynolds number three values 1760, 6160 and 12100 Kumamaru and Fujiwara [4], the following results are made: (a)There is upward displacement. (b)As Reynolds number increases, there is a displacement to the left. (c)As Reynolds number increases, there is an increasing in the velocity range. See (figures 5). Effect of Hartmann number, To study the effect of Hartmann number on the velocity distribution, we keep Reynolds number and time fixed at 6160, Pi/6 and we give Hartmann number three values 169, 269 and 569 Kumamaru and Fujiwara [4], the following results are made: (a) There is upward displacement. (b)As Hartmann number increases, there is a displacement to the left. (c)As Hartmann number increases, there is an increasing in the velocity range. See (figures 6). Effect of time, To study the effect of time on the velocity distribution, we keep Reynolds and Hartmann numbers fixed at 1760 and 169, respectively, Kumamaru and Fujiwara [4], and time will be varies from π/200 to π/100, the following results are made: (a) There is upward displacement. (b)As time increases, there is no displacement to right or left,since γ dose not change. (c)As time increases, there is a small increasing in the velocity range. See (figures 7).

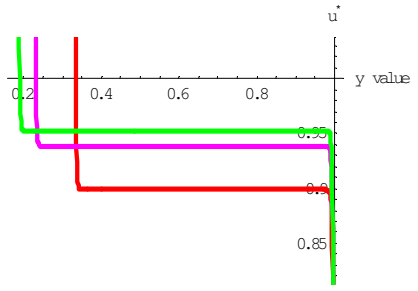

Figure 5: Ha = 469, t = Pi/4, Re = 1760, 6160, 12100.

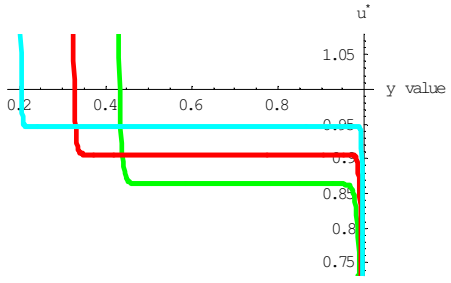

Figure 6: Re=6160,t=Pi/6, Ha=169, 269,569

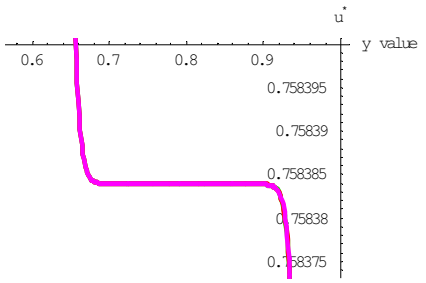

Figure 7: Re = 1760, Ha = 169, t = Pi/200, Pi/150, Pi/100.

3.2 Temperature Distribution of Model 1

In this section, we have studied the effect of each of Reynolds, Hartmann, Prandtl numbers, $\frac{\partial\theta}{\partial z^*}$, and time will be considered also.

Effect of Reynolds number, To study the effect of Reynolds number on the temperature distribution, we keep Hartmann, Prandtl, $\frac{\partial\theta}{\partial z^*}$ and time fixed at 469, 0.694, 1 and 5π/4 respectively, while Reynolds will be given three values 1760, 6160 and 12100 [4], Bayazitoğlu and Özişik [1], and Gebhert [3], following results are observed: (a) There is downward displacement. (b) As Reynolds number increases, there is a displacement to the left. (c) As Reynolds number increases, there is a decreasing in the temperature range. See (figures 8). Effect of Hartmann number, To study the effect of Hartmann number on the temperature distribution, we keep each of Reynolds, Prandtl numbers, $\frac{\partial\theta}{\partial z^*}$ and time Pi/6 fixed at 1760, 0.694 and 1, respectively, while Hartmann will be given three values 269, 369 and 469 Kumamaru and Fujiwara [4], Bayazitoğlu and Özişik [1] and Giebhert [3], the following results are made: (a)There is downward displacement. (b) As Hartmann number increases, there is a displacement to the left. (c) As Hartmann number increases, there is a small decreasing in the temperature range. See (figures 9). Effect of Prandtl number. To study the effects of Prandtl number on the temperature distribution, we keep Hartmann, $\frac{\partial\theta}{\partial z^*}$, Reynolds and time fixed at 169, 1, 6160, and π/4, respectively, while Prandtl number will be given two values 0.694 and 0.71, Kumamaru and Fujiwara [5], Bayazitoğlu and Özişik [1], and Gebhert [3], the following results are observed: (a) There is a small downward displacement. (b) As Prandtl number increases, there is no displacement to right or left, since γ dose not change. (c) As Prandtl number increases, there is a small decreasing in the temperature range. See (figures 10). Effect of $\frac{\partial\theta}{\partial z^*}$, The term $\frac{\partial\theta}{\partial z^*}$ will effect the temperature range only. And effect of time, To study the effect of time on temperature distribution, we keep each of Reynolds, Hartmann, Prandtl numbers and $\frac{\partial\theta}{\partial z^*}$ are the fixed values 12100, 169, 0.71 and 1, respectively, Kumamaru and Fujiwara [5], Bayazitoğlu and Özişik [6] and Gebhert [7], while time varies between π/384 and π/96, the following results are observed: (a) There is very small upward displacement. (b) As time increases, there is no displacement to right or left, since γ dose not change. (c) As time increases, there is a small decreasing in the temperature range. See (figures 11).

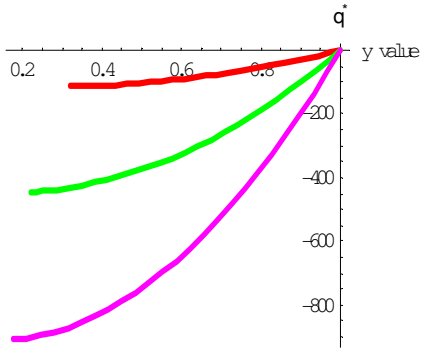

Figure 8: Ha=469,Pr=0.694, $\frac{\partial\theta}{\partial z^*}$ =1, t=5Pi/4, Re= 1760, 6160, 12100.

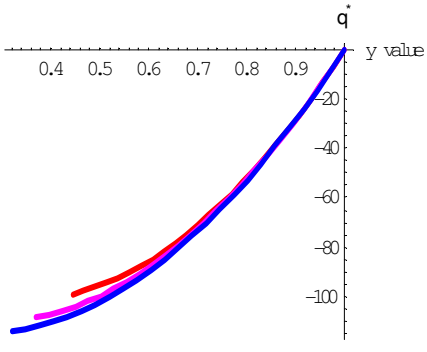

Figure 9: Re = 1760, Pr = 0.694, $\frac{\partial\theta}{\partial z^*}$ = 1, t = Pi/6, Ha = 269,369,469.

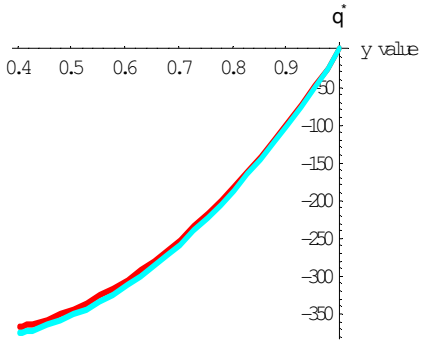

Figure 10: Re = 6160, Ha = 169, $\frac{\partial \theta}{\partial z^*}$ = 1, t = Pi/4, Pr = 0.694, 0.71.

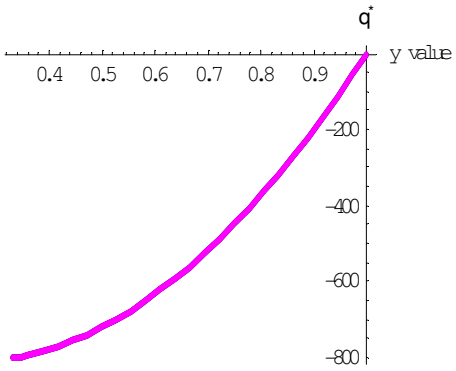

Figure 11: Re = 12100, Ha = 169, $\frac{\partial \theta}{\partial z^*}$ = 1, Pr = 0.71, t = Pi/384, Pi/192, Pi/96.

3.3 Velocity Distribution of Model 2

In this section, we have studied the effect of Reynolds, Hartmann numbers, and time will be considered also.

Effect of Reynolds number. To study the effect of Reynolds number on the velocity distribution, we keep Hartmann number and time fixed at 469, Pi/4 and we give Reynolds number three values 1760, 6160 and 12100 Kumamaru and Fujiwara [4], the following results are made: (a) As Reynolds number increases, there is a displacement to the left. (c) As Reynolds number increases, there is no increasing or decreasing in the velocity range. This is because p = p', since Ha dose not change in three cases. See (figures 12). Effect of Hartmann number, To study the effect of Hartmann number on the velocity distribution, we keep Reynolds number and time fixed at 6160,Pi/6 and we give Hartmann number three values 169, 269 and 569 Kumamaru and Fujiwara [4], the following results are made: (a) There is downward displacement. (b)As Hartmann number increases, there is a displacement to the left. (c) As Hartmann number increases, there is a decreasing in the velocity range. See (figures 13). Effect of time, To study the effect of time on the velocity distribution, we keep Reynolds and Hartmann numbers fixed at 1760 and 169, respectively, Kumamaru and Fujiwara [4], and time will be varies from π/10000 to π/1000, the following results are made: (a) There is upward displacement. (b) As time increases, there is no displacement to right or left, since γ dose not change. (c) As time increases, there is an increasing in the velocity range. See (figures 14).

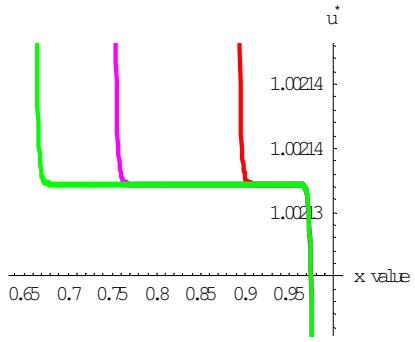

Figure 12: Ha=469, t=Pi/4, Re= 1760, 6160, 12100.

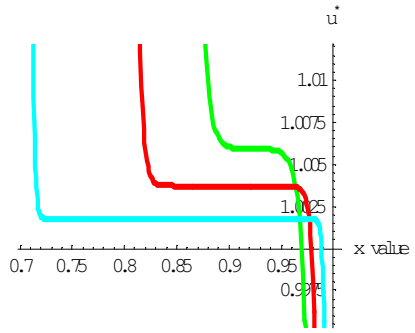

Figure 13: Re=6160, t=Pi/6, Ha=169, 269, 569.

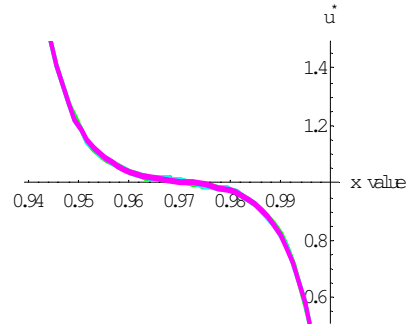

Figure 14: Re=1760, Ha=169, t=Pi/10000, Pi/9000, Pi/1000.

3.4 Temperature Distribution of Model 2

In this section, we have studied the effect of each of Reynolds, Hartmann, Prandtl numbers, $\frac{\partial\theta}{\partial z^*}$, and time will be considered also.

Effect of Reynolds number, To study the effect of Reynolds number on the temperature distribution, we keep Hartmann, Prandtl, $\frac{\partial\theta}{\partial z^*}$ and time fixed at 469, 0.694, 1 and $5\pi/4$, respectively, while Reynolds will be given three values 1760, 6160 and 12100 Kumamaru and Fujiwara [4], Bayazitoğlu and Özişik [6], and Gebhert [7], following results are observed: (a) There is downward displacement. (b) As Reynolds number increases, there is a displacement to the left. (c) As Reynolds number increases, there is a decreasing in the temperature range. See (figures 15). Effect of Hartmann number, To study the effect of Hartmann number on the temperature distribution, we keep each of Reynolds, Prandtl numbers and $\frac{\partial\theta}{\partial z^*}$ fixed at 1760, 0.694, Pi/6 and 1, respectively, while Hartmann will be given three values 269, 369 and 469 Kumamaru and Fujiwara [4], Bayazitoğlu and Özişik [6] and Giebhert [7], the following results are made: (a) There is downward displacement. (b) As Hartmann number increases, there is a displacement to the left. (c) As Hartmann number increases, there is a decreasing in the temperature range. See (figures 16). Effect of Prandtl number. To study the effects of Prandtl number on the temperature distribution, we keep Hartmann, $\frac{\partial\theta}{\partial z^*}$, Reynolds and time fixed at 169, 1, 6160, and $\pi/4$, respectively, while Prandtl number will be given two values 0.694 and 0.71, Kumamaru and Fujiwara [4], Bayazitoğlu and Özişik [7], and Gebhert [6], the following results are observed: (a) There is a small downward displacement. (b) As Prandtl number increases, there is no displacement to right or left, since γ dose not change. (c) As Prandtl number increases, there is a small decreasing in the temperature range. See (figures 17). Effect of $\frac{\partial\theta}{\partial z^*}$, The term $\frac{\partial\theta}{\partial z^*}$ will effect the temperature range only. And effect of time, To study the effect of time on temperature distribution, we keep each of Reynolds, Hartmann, Prandtl numbers and $\frac{\partial\theta}{\partial z^*}$ are the fixed values 12100, 169, 0.71 and 1, respectively, Kumamaru and Fujiwara [4], Bayazitoğlu and Özişik [7] and Gebhert [6], while time varies between $\pi/1500$ and π, the following results are observed: (a) There is downward displacement. (b) As time increases, there is no displacement to right or left, since γ dose not change. (c) As time increases, there is a decreasing in the temperature range. See (figures 18).

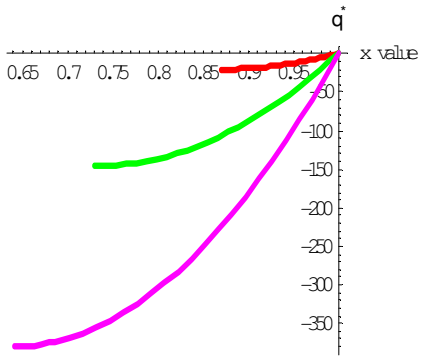

Figure 15: Ha=469,Pr=0.694, $\frac{\partial\theta}{\partial z^*}$=1, t=5Pi/4, Re= 1760, 6160, 12100.

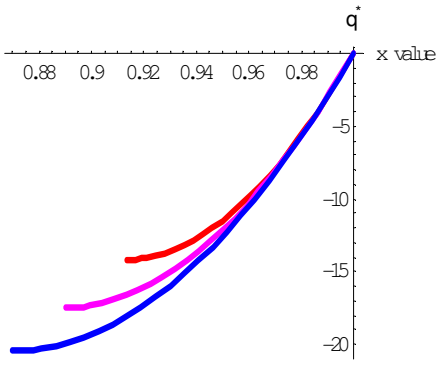

Figure 16: Re=1760,Pr=0.694, $\frac{\partial\theta}{\partial z^*}$=1, t=Pi/6, Ha= 269,369, 469.

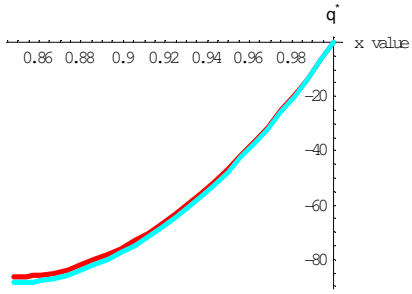

Figure 17: Re=6160,Ha=169, $\frac{\partial\theta}{\partial z^*}$=1, t=Pi/4, Pr= 0.694, 0.71.

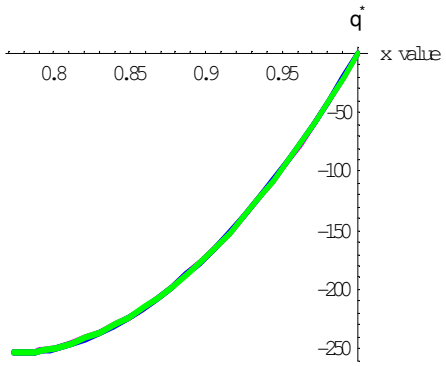

Figure 18: Re=12100,Ha=169, $\frac{\partial\theta}{\partial z^*}$=1, Pr=0.71, t=Pi/1500, Pi/500, Pi.

References

1. Thome R. J. **1964**. Effect of a Transverse Magnetic Field on Vertical Two-Phase Flow Through a Rectangular Channel. *Argonne Nationl Laboratory Report* ANL-6854.
2. Owen, R. G., Hunt, J. C. R., and Collier, J. G. **1975**. Magnetohydrodynamics Pressure Drop in Ducted Two-Phase Flows. *Int. J. Multiphase Flow,* Vol.**3**, pp.23-33.
3. Inoue, A., Aritomi, M., Takahashi, M., Narita, Y., Yano, T., and Matsuzaki, M. **1987**. Studies on Magnetohydrodynamics (MHD) Pressure Drop and Heat Transfer of Helium-Lithium Annular-Mist Flow in a Transverse Magnetic Field. *JSME International Journal,* Vol,**30**, No.267, pp.1768-1775.
4. Kumamaru H., and Fujiwara Y. **1998**. Pressure Drop and Heat Transfer of Magnetohydrodynamics Annular Two-Phase Flow in Rectangular Channel. *Journal of Fluid Engineering*, Vol.**120**, MARCH, pp.152-159.
5. Branover H. **1978**. *Magnetohydrodynamics Flow in Ducts*. Wiley, New York.p.p.10-30.
6. Bayazitoğlu Y., and Özişik M. N. **1988**. *Elements of Heat Transfer*. McGraw-Hill Book Company, New York.p.p.407-430.
7. Gebhert B. **1993**. *Heat Conduction and Mass Diffusion*. McGraw-Hill, Inc., New York.p.p.1-90.
8. Lielausis, O.,**1975**.Liquid Metal Magnetohydrodynamics. *Atomic Energy Review*, Vol.**13**, pp.527-581.